Carbon−Carbon Triple Bonds as Nucleophiles: Adducts of Ethyne and Propyne with Boron Trifluoride

W. A. Herrebout,[†] J. Lundell,[‡] and B. J. van der Veken*,[†]

Department of Chemistry, Universitair Centrum Antwerpen, Groenenborgerlaan 171, B-2020 Antwerp, Belgium, and Laboratory of Physical Chemistry, Department of Chemistry, P.O. Box 55 (A.I. Virtasen aukio 1), FIN-00014 University of Helsinki, Finland

Received: June 17, 1999; In Final Form: July 6, 1999

The mid-infrared (4000−400 cm^{-1}) spectra of ethyne/BF_3 and propyne/BF_3 mixtures, dissolved in liquefied argon are discussed. In all spectra, the formation of a 1:1 van der Waals complex was observed, while at higher concentrations of BF_3 absorption bands of a 1:2 species between propyne and BF_3 were also observed. Using spectra recorded at several temperatures between 96 and 125 K, the complexation enthalpy $\Delta H°$ for ethyne·BF_3 was determined to be −9.3(4) kJ mol^{-1}. For propyne·BF_3 and propyne·$(BF_3)_2$ the $\Delta H°$ values are −13.2(4) and −19.8(12) kJ mol^{-1}, respectively. For the 1:1 complexes the structures and harmonic vibrational frequencies were calculated at the MP2/6-31+G(d) level, while for the 1:2 adduct similar calculations were carried out at the corresponding RHF level. Using a SCRF/SCIPCM scheme to correct for the solvent influences, and statistical thermodynamics to account for the zero-point vibrational and thermal contributions, approximate values for the gas-phase complexation energy were obtained from the experimental enthalpies. The resulting values, −14.3(10) kJ mol^{-1} for ethyne·BF_3, −18.9(10) kJ mol^{-1} for propyne·BF_3, −30.5(12) kJ mol^{-1} for propyne·$(BF_3)_2$, are compared with the ab initio values.

Introduction

The π bonds of unsaturated molecules are regions of high electron density. As a consequence, these molecules are nucleophiles, and they can be expected to form adducts with electrophiles. The π bond systems are classified as soft bases in the HSAB Principle,[1] and, consequently, their adducts with hard acids will be weak. While the structures and properties of strong adducts are well-documented, weak complexes have been much less investigated. It is in the latter field that the present study must be situated. Boron trifluoride is a typical hard acid, whose complexes with ethene and propene have recently been reported for the first time.[2] In agreement with expectations, the complexation energy in the vapor phase was found to be low, estimated at −14.2(2) kJ mol^{-1} for ethene·BF_3, and at −16.3(2) kJ mol^{-1} for propene·BF_3.[2] Molecules containing carbon−carbon triple bonds will also be soft bases, with a softness similar to that of C═C double bonds. Up to now, however, no adducts of such molecules with boron trifluoride appear to have been reported. Therefore, in this study we have investigated if such complexes can be detected. For simplicity, the lower two homologues, ethyne and propyne, were selected as nucleophiles. In view of the expected weakness of the complexes, their formation was studied at low temperatures, in liquid argon (LAr) and liquid nitrogen (LN_2), using infrared spectroscopy to detect the species. In the following paragraphs we will describe the spectra observed, and it will be shown that complexes with BF_3 indeed are formed. Their stoichiometry and complexation enthalpy will be reported and, in addition, structural and spectral information obtained from ab initio calculations will be discussed.

* Corresponding author. E-mail: bvdveken@ruca.ua.ac.be.
[†] Universitair Centrum Antwerpen.
[‡] University of Helsinki.

Experimental Section

The samples of propyne (99%) and boron trifluoride (CP grade) were purchased from Praxair and Union Carbide, respectively. The ethyne was synthesized in small amounts by hydrolyzing CaC_2 with H_2O and was purified by pumping the reaction mixture through a 2-propanol slush (180 K), followed by fractionation on a low-temperature, low-pressure fractionation column. The solvent gases, argon and nitrogen, were supplied by L′Air Liquide and have a stated purity of 99.9999%. In the spectra of ethyne, argon, and nitrogen, no impurities could be detected, while minute amounts of SiF_4 were present in BF_3, and 1,2-propadiene (allene) was detected as an impurity in the propyne used. All gases were used without further purification.

The infrared spectra were recorded on a Bruker IFS 66v or a Bruker 113v Fourier Transform spectrometer, using a Globar source in combination with a Ge/KBr beam splitter and a broadband MCT detector. The interferograms were averaged over 200 scans, Happ Genzel apodized, and Fourier transformed using a zero filling factor of 4 to yield spectra at a resolution of 0.5 cm^{-1}.

A detailed description of the liquid noble gas setup has been given before.[3] To be able to distinguish the spectra of dissolved and undissolved species, the solid-state spectra of ethyne and propyne were obtained by condensing a small amount of the compound onto a CsI window, cooled to 10 K using a Leybold Heraeus ROK 10−300 cooling system, followed by annealing until no further changes were observed in the infrared spectrum.

Computational Details

Ab initio calculations were performed using *Gaussian 94*.[4] For all calculations, second-order Møller−Plesset perturbation theory was used including explicitely all electrons, while a 6-31+G(d) basis set was used.

10.1021/jp992010w CCC: $18.00
Published on Web 09/08/1999

TABLE 1: Observed Vibrational Frequencies and Complexation Shifts (cm^{-1}) for C_2H_2, $^{10}BF_3$, $^{11}BF_3$, $C_2H_2 \cdot ^{10}BF_3$, and $C_2H_2 \cdot ^{11}BF_3$ Dissolved in Liquid Argon at 100 K

	$^{11}BF_3$	$C_2H_2 \cdot ^{11}BF_3$		$^{10}BF_3$	$C_2H_2 \cdot ^{10}BF_3$	
BF_3 submolecule[a]	$\bar{\nu}$	$\bar{\nu}$	$\Delta\bar{\nu}$	$\bar{\nu}$	$\bar{\nu}$	$\Delta\bar{\nu}$
$2\nu_3^{BF_3}$	2887.3	2873.3	−14.0	2989.8	2975.8	−14.0
$\nu_1^{BF_3} + \nu_3^{BF_3} + \nu_4^{BF_3}$	2799.1	2787.0	−12.1	2851.0		
$\nu_1^{BF_3} + \nu_3^{BF_3}$	2325.6	2313.0	−12.6	2375.8	2362.9	−12.9
$2\nu_1^{BF_3} + \nu_4^{BF_3}$	2235.9	2224.5	−11.4	2235.9	2224.5	−11.4
$\nu_3^{BF_3} + \nu_4^{BF_3}$	1922.5	1914.5	−8.0	1974.2		
$\nu_1^{BF_3} + 2\nu_4^{BF_3}$	1833.5	1825.5	−8.0	1833.5	1825.5	−8.0
$\nu_3^{BF_3}$	1445.0	1438.0	−7.0	1494.1	1487.1	−7.0
$\nu_1^{BF_3} + \nu_4^{BF_3}$	1357.7	1351.3	−6.4	1357.7	1351.3	−6.4
$\nu_1^{BF_3}$	*b*	878.5		*b*	878.5	
$\nu_2^{BF_3}$	679.6	651.8	−27.8	712.6	c	
$\nu_4^{BF_3}$	474.0	473.1	−0.9	474.0	473.1	−0.9

	C_2H_2	$C_2H_2 \cdot BF_3$	
C_2H_2 submolecule[d]	$\bar{\nu}$	$\bar{\nu}$	$\Delta\bar{\nu}$
$\nu_2^{C_2H_2} + \nu_5^{C_2H_2}$	2701.7	2715.4	+13.7
		2706.4	+4.7
$\nu_2^{C_2H_2}$	*d*	1970.1	−3.9
$\nu_4^{C_2H_2} + \nu_5^{C_2H_2}$	1327.2	1338.6	+11.4
$\nu_5^{C_2H_2}$	731.3	747.5	+16.2
$\nu_4^{C_2H_2}$	595.9	591.1	−4.8

[a] The BF_3 normal modes are identified as follows: ν_1 is the BF_3 symmetric stretch, ν_2 is the BF_3 out of plane deformation, ν_3 is the BF_3 antisymmetric stretch, ν_4 is the BF_3 in plane deformation. [b] Not infrared-active, Raman gas-phase frequency at 888 cm^{-1}. [c] Due to the overlap with the 679.6 cm^{-1} band, no accurate frequency could be determined for the $\nu_2^{BF_3}$ mode in $C_2H_2 \cdot ^{10}BF_3$. [d] Not infrared-active, Raman gas-phase frequency at 1974 cm^{-1}.

The complexation energies of the complexes were calculated by subtracting the calculated energies of the monomers from that of the complex, and these energies were corrected for basis set superposition error (BSSE) using the counterpoise correction method described by Boys and Bernardi.[5] For all equilibrium geometries, the vibrational frequencies and the corresponding infrared intensities were calculated using harmonic force fields.

The calculations were carried out on the Cray C94 supercomputer at the CSC−Center for Scientific Computing Ltd (Espoo, Finland) and on a Digital Alpha workstation.

Results

Vibrational Spectra. *A. Monomers.* The vibrational spectra of boron trifluoride in LAr have been described in detail elsewhere.[6,7] In contrast, no infrared data of ethyne or propyne in cryosolutions have been reported. Therefore, the vibrational frequencies of these species observed for a solution in LAr at 100 K, are summarized in Tables 1S and 2S of the Supporting Information. The assignments given in the tables are based on those in the vapor phase.[8−10] In the tables the fundamentals are numbered according to the Herzberg system. For the complexes we will use the same numbering, using the chemical formula of the species in which the mode is localized, as a superscript.

B. Ethyne/BF_3. In the spectra of ethyne/BF_3 mixtures dissolved in LAr, new bands were observed in the vicinity of the monomer bands. This proves that in the solutions a complex is formed. Due to the limited solubility of ethyne, it was not possible to derive the stoichiometry of the complex from a concentration study.[2] However, on statistical grounds, the 1:1 adduct $C_2H_2 \cdot BF_3$ is the most likely complex to be formed and therefore, we assign the observed complex bands to this species. The frequencies of these bands, their assignments, and complexation shifts are summarized in Table 1.

In Figure 1S of the Supporting Information the formation of the complex is illustrated using the $\nu_1^{BF_3} + \nu_3^{BF_3}$ region of the spectra. For the mixture new bands appear at 2362.9 and 2313.0 cm^{-1}, on the low-frequency side of the monomer bands at 2375.8 and 2325.6 cm^{-1}, which are due to $^{10}BF_3$ and $^{11}BF_3$, respectively. Similarly, complex bands were found for $\nu_3^{BF_3}$, red-shifted from 1494.1 to 1487.1 cm^{-1} (^{10}B isotopomer) and from 1445.0 to 1378.0 cm^{-1} (^{11}B isotopomer), while for the $^{11}BF_3$ out-of-plane deformation modes $\nu_2^{BF_3}$, a band red-shifted by approximately 28 cm^{-1} was observed.

Upon complexation with BF_3, the $\nu_5^{C_2H_2}$ fundamental at 731.3 cm^{-1} and the $\nu_4^{C_2H_2} + \nu_5^{C_2H_2}$ combination at 1327.2 cm^{-1} give rise to blue-shifted complex bands, at 747.5 and 1338.6 cm^{-1}, respectively. Moreover, on the high-frequency side of the monomer band at 2701.7 cm^{-1}, assigned to $\nu_2^{C_2H_2} + \nu_5^{C_2H_2}$, a weak doublet due to the 1:1 adduct is observed, with maxima at 2715.4 and 2706.4 cm^{-1}, respectively. The observation of a doublet can only be the consequence of the lifting of the degeneracy of $\nu_5^{C_2H_2}$ upon complexation. But then also the fundamental $\nu_5^{C_2H_2}$ in the complex must be a doublet, and this is not obvious from the spectra. A possible explanation for this is offered by the ab initio calculations (vide infra, Table 6S), which suggest that the second component occurs in the immediate vicinity of monomer $\nu^{C_2H_2}$, which presumably hides it.

The observation of weak complex bands due to modes that are symmetry-forbidden in the monomers is not uncommon.[2,11] Also for $C_2H_2.BF_3$ such bands may appear, and, to this end, saturated solutions of BF_3 and C_2H_2 were investigated. The regions of and $\nu_2^{C_2H_2}$ and $\nu_1^{BF_3}$ of these spectra are shown in Figures 1, parts A and B, respectively. In each region a new band is detected for the mixture. The observed frequencies, 1970.1 and 875.5 cm^{-1}, are sufficiently close to the gas-phase Raman frequencies of the monomer modes involved to warrant their assignment to the induced modes in the complex. Another candidate would be $\nu_1^{C_2H_2}$. However, a close inspection of the corresponding spectral region has not revealed the presence of

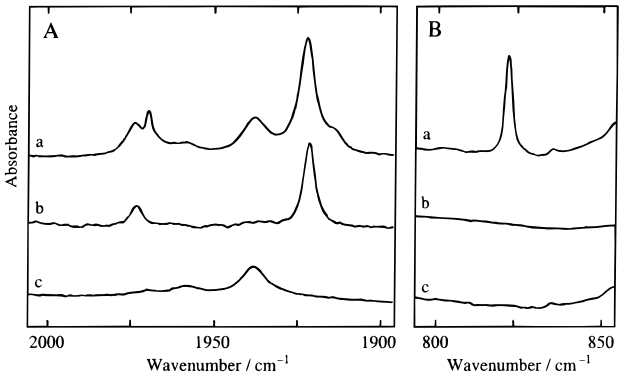

Figure 1. The $\nu_2^{C_2H_2}$ (A) and $\nu_1^{BF_3}$ (B) region of the spectra of solutions in liquid argon, at 100 K: (a) solution containing both C_2H_2 and BF_3; (b) solution containing only BF_3; (c) solution containing only C_2H_2.

TABLE 2: Observed Vibrational Frequencies and Complexation Shifts (cm^{-1}) for C_3H_4, $^{10}BF_3$, $^{11}BF_3$, C_3H_4·$^{11}BF_3$, C_3H_4·$^{10}BF_3$, and $^{11}BF_3$ Dissolved in Liquid Argon at 100 K

	$^{11}BF_3$	C_3H_4·$^{11}BF_3$		$^{10}BF_3$	C_3H_4·$^{10}BF_3$	
BF_3 submolecule[a]	$\bar{\nu}$	$\bar{\nu}$	$\Delta\bar{\nu}$	$\bar{\nu}$	$\bar{\nu}$	$\Delta\bar{\nu}$
$\nu_1^{BF_3} + \nu_3^{BF_3}$	2325.1	2304.8	−20.3	2376.2	2354.4	−20.8
$\nu_3^{BF_3}$	1444.8	1433.0	−11.8	1496.3	1484.5	−11.8
$\nu_1^{BF_3} + \nu_4^{BF_3}$	1358.2	1347.6	−10.6	1358.2	1347.6	−10.6
$\nu_1^{BF_3}$	*a*	875.3		*a*	875.3	
$\nu_2^{BF_3}$	680.4	643.1	−37.5	707.9	672.1	−35.8

	C_3H_4	C_3H_4·BF_3	
C_3H_4 submolecule	$\bar{\nu}$	$\bar{\nu}$	$\Delta\bar{\nu}$
$\nu_1^{C_3H_4}$	3328.9	3322.8	−6.1
$\nu_3^{C_3H_4}$	2138.5	2134.2	−4.3
$2\nu_9^{C_3H_4}$	1250.1	1257.1	+7.0
		1292.0	+41.9
$\nu_9^{C_3H_4}$	630.2	659.1	+29.1

[a] Not infrared-active, Raman gas-phase frequency at 888 cm^{-1}.

an induced band, so it must be concluded that this mode in the complex is extremely weak.

C. Propyne/BF₃. Also for C_3H_4/BF_3 mixtures dissolved in LAr new bands are observed near monomer bands of both C_3H_4 and BF_3, signaling that a complex is formed. The observed frequencies, their assignments and the complexation shifts are summarized in Table 2.

In Figure 2S, several spectral regions of mixed solutions are compared with those of the monomers. In the $\nu_3^{BF_3}$ region, Figure 2S(B), of the mixed solutions, complex bands are observed at 1484.5 and 1433.0 cm^{-1}. Meanwhile, on the low-frequency side of the $\nu_2^{BF_3}$ isotopic doublet, shown in Figure 2S(C), complex bands appear at 672.1 and 643.1 cm^{-1}.

Figure 2S(A), giving the region of $\nu_1^{BF_3} + \nu_3^{BF_3}$, shows that also for propyne/BF_3 mixtures complex bands are observed for the combination bands involving $\nu_2^{BF_3}$ or $\nu_3^{BF_3}$.

For $\nu_9^{C_3H_4}$ and $2\nu_9^{C_3H_4}$, assigned in the monomer at 630.2 and 1250.1 cm^{-1}, complex bands appear at 659.1, 1257.1, and 1292.0 cm^{-1}. Just as for $\nu_5^{C_2H_2}$ in the ethyne complex, the occurrence of a doublet for $2\nu_9$ proves that the degeneracy of ν_9 in the complex is lifted. The absence of a complex doublet for the fundamental transition also here is explained by the ab initio calculations (vide infra, Table 7S), which predict that, as for $\nu_5^{C_2H_2}$, one of the components of ν_9 in the complex occurs nearly accidentally degenerate with the monomer ν_9 band.

TABLE 3: Complexation Energies (kJ mol^{-1}) for C_2H_2·BF_3 and C_3H_4·BF_3

	C_2H_2·BF_3	C_3H_4·BF_3
MP2/6-31+G(d)		
ΔE	−16.25	−22.62
E_{BSSE}	−9.44	−13.07
ΔE_c	−6.81	−9.55
MP2/6-311++G(3df,2pd)//MP2/6-31+G(d)		
ΔE	−15.31	−19.25
E_{BSSE}	−5.83	−4.98
ΔE_c	−9.68	−14.26
MP2/aug-cc PVTZ//MP2/6-31+G(d)		
ΔE	−20.95	−23.31
E_{BSSE}	−9.13	−8.76
ΔE_c	−11.80	−14.55
Experimental values		
ΔH°_{LAr}	−9.3(4)	−13.2(4)
ΔH°_{gas}[a]	−12.2(4)	−16.6(4)
ΔE_c^{gas}[b]	−14.3(4)	−18.9(4)

[a] Obtained by using the SCRF/SCIPCM solvent destabilization energies calculated at the RHF/6-311+G(d) level. [b] Obtained by correcting for zero-point vibrational and thermal influences.

TABLE 4: Van der Waals Bond Lengths and Dissociation Energies for ethyne·BF_3 and propyne·BF_3 Derived Using RHF/6-311++G(2d,2p) Distributed Multipole Moments and Lennard-Jones Atom-Atom Potentials

	calculation 1[a]	calculation 2[a]
ethyne·BF_3		
ΔE/kJ mol^{-1}	−15.43	−17.95
$R_{X\cdots B}$/Å	2.97	2.92
propyne·BF_3		
ΔE/kJ mol^{-1}	−26.09	−25.15
$R_{X\cdots B}$/Å	2.87	2.93

[a] Calculation 1: results obtained using point charges, dipoles, and quandrupoles; calculation 2: results obtained using point charges, dipoles, quadrupoles, and octupoles.

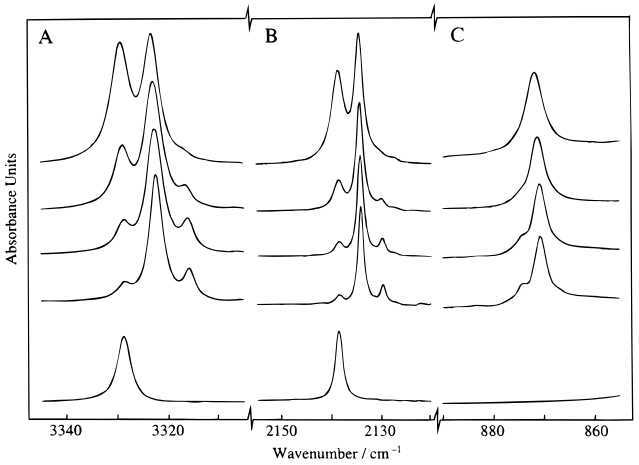

Figure 2. $\nu_1^{C_3H_4}$(A), and $\nu_3^{C_3H_4}$ (B) and $\nu_1^{BF_3}$ (C) regions for a solution in liquid argon containing C_3H_4 and BF_3. The bottom spectra were recorded from a solution containing only C_3H_4. For the other spectra, the temperatures of the solution are, from top to bottom, 116, 111, 106, and 101 K.

Figure 2 illustrates the temperature dependence of the complex bands in the regions of $\nu_1^{C_3H_4}$, (A) and $\nu_3^{C_3H_4}$, (B) $\nu_1^{BF_3}$, for a solution in LAr for which the mole fractions of C_3H_4 and BF_3 are 3×10^{-5} and 7.5×10^{-5}, respectively. It can be seen that for $\nu_1^{C_3H_4}$ and for $\nu_3^{C_3H_4}$ a second complex band becomes clearly visible at lower temperatures, while for these modes no lifting of degeneracy is involved. The spectra in Figure 2 have been drawn in such a way that the absorbance of the more intense complex band is the same at all temperatures, and it

can be seen that lowering the temperature increases the absorbance of the second complex band. This shows that the first and second complex band in each region arise in different complexes. As similar behavior is observed for isothermal concentration studies, the stoichiometry of the complexes must be different. These stoichiometries were determined as described before,[2] from a concentration study. In this, solutions in LAr containing mole fractions of C_3H_4 varying between 0.9×10^{-5} and 6.6×10^{-5}, and of BF_3 varying between 0.6×10^{-5} and 15×10^{-5}, were investigated at a constant temperature of 105.9(5) K. Intensities for monomer propyne and the complexes were taken from least squares band fittings of the $\nu_1^{C_3H_4}$ region, and for BF_3 the integrated intensity of the 2376.2 cm^{-1} was used. Using these, plots were made of the intensities of the complex bands at 3322.6 and 3316.3 cm^{-1} versus the intensity products $(I_{BF_3})^2 \times I_{C_3H_4}$ (a), $I_{BF_3} \times I_{C_3H_4}$ (b), and $I_{BF_3} \times (I_{C_3H_4})^2$. The χ^2 values for the linear regressions on these plots are given in Table 3S. It is clear from these data that for the 3322.6 cm^{-1} band the highest linearity is obtained for product (b), and for product (a) in the case of the 3316.3 cm^{-1} band. This shows that the former arises in a 1:1 complex $C_3H_4 \cdot BF_3$, and the latter in a 1:2 complex $C_3H_4 \cdot (BF_3)_2$. Finally, Figure 2C gives the region of $\nu_1^{BF_3}$. Also here, two induced bands are visible at the lowest temperatures. Consistent with the above results, the stronger one, at 875.3 cm^{-1}, is assigned to the 1:1 complex, the weaker one, at 877.5 cm^{-1}, to the 1:2 complex.

Complexation Enthalpy of the Observed Species. Using the Van't Hoff isochore,[12] it can be shown that $\ln[I_{C_xH_y \cdot (BF_3)_n} / I_{C_xH_y} \times (I_{BF_3})^n]$ is linearly related to $1/T$, and that the slope of this relation equals $-\Delta H^\circ/R$, in which ΔH° is the complexation enthalpy. To establish the complexation enthalpy of $C_2H_2 \cdot BF_3$, $C_3H_4 \cdot BF_3$, and $C_3H_4 \cdot (BF_3)_2$, the spectra of several $C_2H_2 \cdot BF_3$ and $C_3H_4 \cdot BF_3$ mixtures in LAr were recorded at different temperatures between 96 and 125 K. At temperatures below 107 K, a large fraction of the ethyne molecules crystallizes and so only very weak absorption bands due to dissolved C_2H_2 and $C_2H_2.BF_3$ are observed. Because such spectra do not allow a precise quantitative analysis, they were not used in the analysis.

Also this analysis requires the integrated intensities of a band of each species involved in the equilibrium. For $C_2H_2 \cdot BF_3$, the well-separated combination bands in the $\nu_1^{BF_3} + \nu_3^{BF_3}$ region were used to obtain intensities for monomer BF_3 and the complex. Unfortunately, for all modes localized in the ethyne moiety, the complex bands strongly overlap with the monomer modes, making an accurate determination of $I_{C_2H_2}$ rather difficult. For the solutions studied, however, the intensity of the 747.5 cm^{-1} band, assigned to the 1:1 complex, was very small compared to that of the 731 cm^{-1} monomer band. This shows that, even at the lowest tempertures, only a minor fraction of the ethyne molecules are complexed. Then, the contribution of the complex to the 731 cm^{-1} doublet can be neglected without introducing serious error. Therefore, as monomer intensity $I_{C_2H_2}$ the numerically integrated intensity of the 3874.9/3891.0 cm^{-1} doublet was used, without correcting for the presence of complex bands. The resulting Van't Hoff plot for $C_2H_2.BF_3$ is shown in Figure 3a. From the slope of the linear regression, corrected for the density variation of the solution,[12] the complexation enthalpy ΔH° was calculated to be -9.3 kJ mol^{-1}.

Using the integrated intensities of the same monomer and complex bands as in the stoichiometry study described above, Van't Hoff plots for $C_3H_4 \cdot BF_3$ and $C_3H_4 \cdot (BF_3)_2$ were constructed. From these plots, shown in Figure 3, parts b and c, respectively, and accounting for the density variations of the solution,[12] the complexation enthalpies were calculated to be

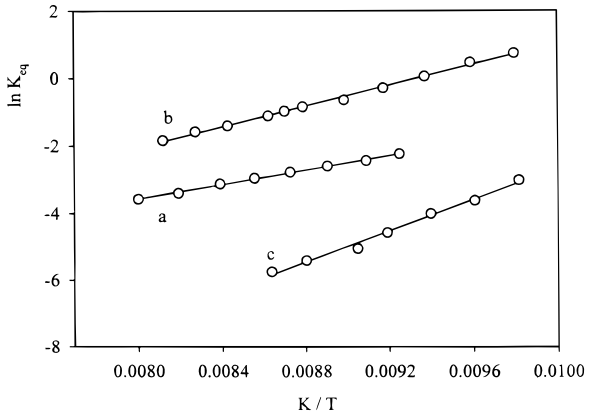

Figure 3. Van't Hoff plots for $C_2H_2 \cdot BF_3$ (a), $C_3H_4 \cdot BF_3$ (b), and $C_3H_4 \cdot (BF_3)_2$ (c) in liquefied argon.

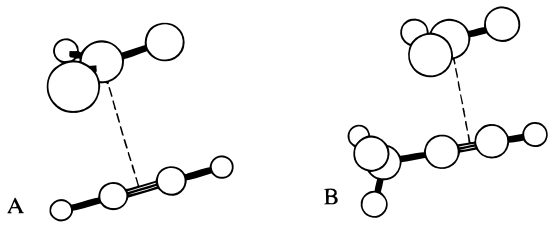

Figure 4. MP2/6-31+G(d) equilibrium geometries for $C_2H_2 \cdot BF_3$ (A) and $C_3H_4 \cdot BF_3$ (B).

$-13.2(4)$ kJ mol^{-1} for $C_3H_4 \cdot BF_3$ and $-19.8(12)$ kJ mol^{-1} for $C_3H_4 \cdot (BF_3)_2$.

Ab Initio Calculations. Insight into the structure of $C_2H_2 \cdot BF_3$ and $C_3H_4 \cdot BF_3$ was gained from ab initio calculations at the MP2/6-31+G(d) level. The resulting equilibrium geometries are shown in Figure 4. The structural parameters are reported in Tables 4S and 5S.

For the 1:1 complexes, we found structures with C_s symmetry, in which the boron atom sits above the π bond of the Lewis base. Therefore, as for ethene$\cdot BF_3$ and propene$\cdot BF_3$, also here the main contribution to the complexation energy must be due to the interaction between the electron-rich π-system and the electron-deficient boron atom. It can be noted from Figure 4, however, that in both complexes one B−F bond is parallel to the R−C≡C−H skeleton. This suggests that a weak interaction between the in-plane F atom and the terminal hydrogen atom of the Lewis base contributes in determining the structure.

A detailed description of the equilibrium geometries requires the definition of a van der Waals bond. For $C_2H_2 \cdot BF_3$, the latter could be defined as the intermolecular distance separating the respective centers of masses of the monomers. A similar analysis for $C_3H_4 \cdot BF_3$, however, is not as straightforward. Therefore, in this study, we defined the van der Waals bond length as the distance between the boron atom and a dummy atom X situated on the line connecting the two carbon atoms of the triple bond, at the perpendicular projection of the boron atom.

From $C_2H_2 \cdot BF_3$ to $C_3H_4 \cdot BF_3$, the distance $R_{X \cdots B}$ decreases slightly, from 2.92 to 2.81 Å, suggesting that the interaction in $C_3H_4 \cdot BF_3$ is slightly stronger than in $C_2H_2 \cdot BF_3$. This is in line with the experimental complexation enthalpies, and with the calculated complexation energies of the complexes.

The complexation has only minor influences on the bond lengths and bond angles of the monomer molecules, and these changes are easily understood from donor−acceptor considerations.[13] The complexation also leads to small deviations from planarity for the BF_3 molecules, and to small deviations from linearity for the R−C≡CH molecular skeletons.

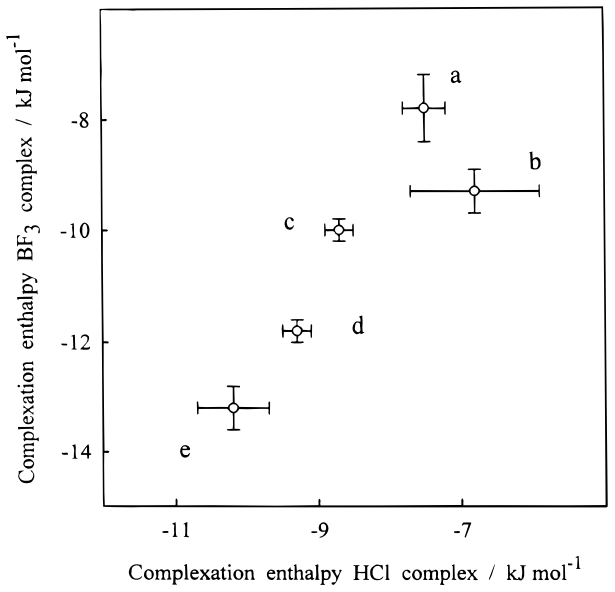

Figure 5. Comparison of the complexation enthalpies $\Delta H°$ for the complexes formed between various Lewis bases, HCl, and BF_3. The Lewis bases studied are (a) cyclopropane, (b) ethyne, (c) ethene, (d) propene, and (e) propyne.

Typical for weakly bound van der Waals complexes are the low barriers hindering internal rotation. The barriers hindering rotation around the van der Waals bond were obtained by systematically varying the required angular parameter, at each value relaxing all other structural parameters. The values, 0.1 kJ mol^{-1} for $C_2H_2 \cdot BF_3$ and 0.05 kJ mol^{-1} for $C_3H_4 \cdot BF_3$, illustrate the extreme nonrigidity of the present complexes.

The vibrational frequencies and infrared intensities of the monomers and the 1:1 complexes calculated at the MP2/6-31G+(d) level, together with the frequency shifts $\Delta\nu = \nu_{\text{complex}} - \nu_{\text{monomer}}$, are given in Tables 6S and 7S. Comparison of calculated with observed shifts shows that in all cases the ab initio calculations predict the correct direction of the shift. However, the agreement is not quantitative. For example, the calculated shifts of the BF_3 fundamentals are significantly larger than the observed ones.

For both $C_2H_2 \cdot BF_3$ and $C_3H_4 \cdot BF_3$, the C_s symmetry of the complexes causes the degenerace of the antisymmetric BF_3 stretches to be lifted. This leads to predicted splittings of 3−5 cm^{-1}. However, things are complicated by the very low internal rotation barrier which makes that the observed antisymmetric stretches are an average over a mixture of initial states, a substantial contribution stemming from molecules excited in torsional levels above the barrier. Instead of giving rise to a well-defined doublet, such an average will collapse into a single, broad band. In agreement with this, for both complexes a single band for these modes is observed.

Discussion

Figure 5 compares the complexation enthalpies of the HCl complexes of ethene,[11] propene,[14] cyclopropane,[14] ethyne,[14,15] and propyne[14] with those of the corresponding BF_3 complexes. It can be seen that the BF_3 complexes systematically have a higher $\Delta H°$, confirming that BF_3 is a stronger Lewis acid than HCl. Except for the ethyne complexes, the data exhibit a high degree of linearity, which shows that the strengths of HCl and BF_3 complexes of unsaturated, or pseudo-unsaturated nucleophiles are closely correlated. If we assume that the correlation must be valid for the ethyne complexes as well, there being no obvious reason it should not, Figure 5 suggests that the reported strength of ethyne/HCl is underestimated by approximately 1.5 kJ mol^{-1} (it may be remarked that the $\Delta H°$ for this complex has the largest uncertainty of the points reported in Figure 5).

The ab initio complexation energies $\Delta E_C^{\text{ab initio}}$ can be compared with experiment if the observed enthalpies are transformed into energies. This was accomplished in two steps. In the first, vapor phase enthalpies $\Delta H°_{\text{gas}}$ were obtained by correcting the solution values for solvation effects. The latter were estimated from Self-Consistent Isodensity Polarizable Continuum Model (SCIPCM) calculations[17] at the RHF/6-311+G* level. The solvation free enthalpies for the monomers resulting from these calculations are collected in Table 8S.

From the free enthalpies, the solvation enthalpies were calculated as described by Stolov et al.,[18] and these were used to transform the liquid phase $\Delta H°$ into the vapor phase value $\Delta H°_{\text{gas}}$. The values found are −12.2 kJ mol^{-1} for $C_2H_2 \cdot BF_3$ and −16.6(4) kJ mol^{-1} for $C_3H_4 \cdot BF_3$.

In the second step, the zero-point and thermal contribution were subtracted from the $\Delta H°_{\text{gas}}$, resulting in complexation energies. These contributions were calculated using standard statistical thermodynamics, from the ab initio vibrational frequencies and rotational constants. The temperature used was 100 K, which is very close to the midpoint of the temperature interval in which the experimental $\Delta H°$ values were determined. The complexation energies ΔE_C^{exp} arrived at are −14.3(10) kJ mol^{-1} for $C_2H_2 \cdot BF_3$ and −18.9(10) kJ mol^{-1} for $C_3H_4 \cdot BF_3$. To account for the approximations used, the uncertainties were taken to be the experimental values multiplied by 2.5.

The uncorrected $\Delta E_C^{\text{ab initio}}$ values calculated at the MP2/6-31+G(d) level overestimate ΔE_C^{exp} by 14% for $C_2H_2 \cdot BF_3$ and 20% for $C_3H_4 \cdot BF_3$, and the BSSE-corrected values are only about half the experimental values. A poor agreement of BSSE-corrected values with experiment has been noted previously[2,16,19] and has been attributed to the fact that for a truncated basis set, such as that used above, the BSSE is largely counterbalanced by the basis set incompleteness error (BSIE).

Both types of error can be decreased by saturating the basis set. Therefore, the complexation energies were obtained from single point calculations at the MP2/6-311++G(3df,2pd) and MP2/aug-cc-PVTZ levels. The resulting values before and after the correction for BSSE, are collected in Table 3. It is clear that enlarging the basis set to 6-311++G(3df,2pd) significantly decreases the BSSE for both complexes. Meanwhile, the corrected complexation energies increase slightly. Comparison with Table 3 shows, however, that even at the MP2/6-311++G-(3df, 2pd) level the corrected values remain significantly smaller than the experimental values.

At the MP2/aug-cc-PVTZ level, the uncorrected complexation energies as well as the BSSE increase, resulting in corrected complexation energies of −11.8 kJ mol^{-1} for $C_2H_2 \cdot BF_3$ and −14.6 kJ mol^{-1} for $C_3H_4 \cdot BF_3$. These results illustrate that Dunning's augmented correlation consistent basis set significantly improves the agreement of the experimental with the BSSE-corrected values, while the agreement with the uncorrected values deteriorates. However, even at this level the corrected values still underestimate the experimental ones by ca. 15%. This is consistent with earlier results[16,18,20,21] which indicate that at the correlated level the BSSE is slightly overcorrected when using the counterpoise correction.

It is widely accepted that van der Waals complexes are held together by electrostatic forces. To see if this applies to the complexes studied here, we have predicted the van der Waals bond lengths and interaction energies for $C_2H_2 \cdot BF_3$ and $C_3H_4 \cdot BF_3$ with a model in which the attractive, electrostatic interactions are balanced by Lennard−Jones atom−atom interaction potentials,[22] as implemented in A. J. Stone's *Orient* program.[23] The electrostatic terms in this model are calculated from distributed multipole expansions of the charge distributions in the monomers. These multipoles were calculated with the *Gamess US* program,[24] at the RHF/6-311++G(2d,2p) level. The convergence of the electrostatic energy was tested by performing the calculation twice, the first time truncating the multipole expansion after the quadrupoles, the second time also including the octupoles.

For both complexes, the calculations resulted in a structure similar to that obtained from the ab initio calculations. The van der Waals bond lengths and complexation energies obtained from these calculations are collected in Table 4. It can be seen that the inclusion of the octupoles changes the complexation energies significantly, showing that convergence presumably requires inclusion of multipoles beyond the octupoles.

Compared with the experimental complexation energies, the relative stability order is correctly predicted, but the stabilities are overestimated by 35−40%. Lacking values for the multipoles beyond the octupoles, it cannot be decided if the differences are inherent to the electrostatic model, or if the nonconvergence of the calculation is to be blamed.

The ab initio dipole moment of $C_2H_2 \cdot BF_3$ is 0.58 D. BF_3 and C_2H_2 having zero dipole moments, the value of the complex can be explained as the sum of two contributions. The first is the structural contribution, arising as a consequence of the nonplanarity of BF_3 and the nonlinearity of C_2H_2 in the complex. The second contribution is due to the moments induced by the multipoles of each monomer in the other.

The structural contributions μ_{BF_3} and $\mu_{C_2H_2}$ were estimated by an ab initio calculation on the monomers, using the geometry they have in the complex. For BF_3, this leads to a dipole moment μ_{BF_3} of 0.18 D, and for C_2H_2 to a value of 0.02 D, both dipole moments nearly parallel to the van der Waals bond. They have been indicated schematically on the right-hand side of Figure 3S. The value for BF_3 can easily be rationalized.[25] By subtracting the structural moments of the monomers from the total dipole moment, the induced contribution is calculated to be 0.39 D, and it is almost parallel to the van der Waals bond. Thus, it is clear that the dipole moment of the complex is caused by structural deformations and induced contributions of similar magnitude.

A similar analysis was performed for the propyne complex. Here, the analysis is slightly more complex, as propyne itself has a moment of 0.77 D. In Figure 3S the different contributions to the dipole moment, $\mu_{complex}$, and their relative orientations are given. It can be seen that also for this complex both structural and induced dipole moments are important.

In addition to the bands assigned to the dimer $C_3H_4 \cdot BF_3$, weak bands due to a trimer species $C_3H_4 \cdot (BF_3)_2$ were observed at 3316.3, 2129.7, and 877.5 cm^{-1}. It is tempting to interpret this complex as one in which the propyne molecule binds to a $(BF_3)_2$ dimer. However, the latter has not been observed in cryogenic solutions up to now. Therefore, we prefer the interpretation that the 1:2 complex has a bifurcated structure in which both the BF_3 molecules bind to the C≡C triple bond. Insight into this complex was again obtained from ab initio calculations. To reduce to an acceptable limit the required computer time, these calculations were performed at the RHF/6-31+G/d) level. The resulting equilibrium geometry is shown in Figure 6. The calculated angle between the two van der Waals bonds is 107.5 degrees. In Table 9S the observed frequency shifts are compared with the calculated values. The agreement is very good, which supports our identification of the observed 1:2 complex.

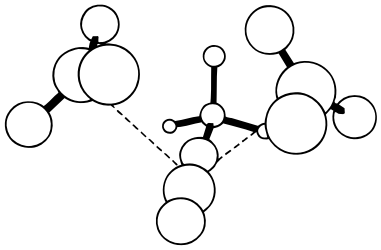

Figure 6. RHF/6-31+G(d) equilibrium geometry for $C_3H_4 \cdot (BF_3)_2$.

The complexation energy of the 1:2 complex was derived from the $\Delta H°$ in LAr by the methods described above, and results in a value of −30.5(12) kJ mol^{-1}, while for the 1:1 complex the value of −18.9(8) kJ mol^{-1} was obtained above. These must be compared with the RHF/6-31+G(d) values, corrected for BSSE, of −12.28 and −6.95 kJ mol^{-1} for the 1:2 and 1:1 complex, respectively. The ab initio values poorly agree with the experimental values, which must be blamed to the relatively limited basis set that were used because of the size of the 1:2 complex. It is clear, however, that for the experimental as well as for the ab initio data the complexation energy for the 1:2 complex is less than twice the value for the 1:1 complex. Hence, an anti-cooperative effect is active, which makes that the addition of a second BF_3 molecule weakens the bond between the nucleophile and the first BF_3 molecule.

Acknowledgment. W.A.H. is indebted to the Fund for Scientific Research (FWO, Belgium) for an appointment as Postdoctoral Fellow. The FWO is also thanked for financial help toward the spectroscopic equipment used in this study. Financial support by the Flemish Community, through the Special Research Fund (BOF), is gratefully acknowledged. The authors thank the CSC—Center for Scientific Computing Ltd. (Espoo, Finland) for computer mainframe time.

Supporting Information Available: Tables 1S and 2S report the observed frequencies, and their assigments, of ethyne and propyne, respectively, dissolved in liquid argon, at 100 K. Table 3S gives the χ^2-values for the stoichiometry analysis of the complexes between propyne and BF_3. In Tables 4S and 5S the MP2/6-31+G(d) structural parameters of the 1:1 complexes of BF_3 with ethyne and propyne, respectively, are compared with those of the monomers. Tables 6S and 7S contain the MP2/6-31+G(d) vibrational frequencies and infrared intensities for the 1:1 complexes of BF_3 with ethyne and propyne, respectively. Table 8S gives the SCRF-SCIPCM solvation enthalpies and free enthalpies for the species studied. In Table 9S the RHF/6-31+G* vibrational frequencies of the monomers and the 1:1 and 1:2 complexes of propyne with BF_3 are compared with the experimental frequencies observed in liquid argon. Figure 1S illustrates the formation of a complex between BF_3 and ethyne in liquid argon, as observed in the 2400−2300 cm-1 region of the infrared spectrum. Figure 2S gives details of the infrared spectra of solutions in liquid argon containing propyne and BF_3. Figure 3S shows the decomposition in structural and induced components of the dipole moment of the 1:1 complexes of BF_3 with etyne and propyne. This material is available free of charge via the Internet at http://pubs.acs.org.

References and Notes

(1) Pearson, R. G. *Inorg. Chim. Acta* **1995**, *240*, 93.
(2) Herrebout, W. A.; Van der Veken, B. J. *J. Am. Chem. Soc*. **1997**, 10446.
(3) Van der Veken, B. J. Infrared Spectroscopy in Liquefied Noble Gases. In *Low-Temperature Molecular Spectroscopy*; Fausto, R., Ed.; Kluwer Academic Publishers: Dordrecht, 1996.
(4) Frisch, M. P.; Trucks, G. W.; Schlegel, H. B.; Gill, P. M. W.; Johnson, B. G.; Robb, M. A.; Cheeseman, J. R.; Keith, T.; Petersson, G. A.; Montgomery, J. A.; Raghavachari, K.; Al-Laham, M. A.; Zakrzewski, V. G.; Ortiz, J. V.; Foresman, J. B.; Cioslowski, J.; Stefanov, B. B.; Nanayakkara, A.; Challacombe, M.; Peng, C. Y.; Ayala, P. Y.; Chen, W.; Wong, M. W.; Andres, J. L.; Replogle, E. S.; Gomperts, R.; Martin, R. L.; Fox, D. J.; Binkley, J. S.; Defrees, D. J.; Baker, J.; Stewart, J. P.; Head-Gordon, M.; Gonzalez, C.; Pople, J. A. *Gaussian 94*, Revision E2; Gaussian, Inc.: Pittsburgh, PA, 1995.
(5) Boys, S. B.; Bernardi, F. *Mol. Phys.* **1970**, *19*, 553.
(6) Sluyts, E. J.; Van der Veken, B. J. *J. Am. Chem. Soc*. **1996**, *118*, 440.
(7) Herrebout, W. A.; Van der Veken, B. J. *J. Am. Chem. Soc.* **1998**, *120*, 9921.
(8) Tesamani, M. A.; Herman, M. *J. Chem. Phys*. **1995**, *102*, 6371.
(9) Herman, M.; Elldussi, M. L.; Disarchik, A.; Dilonardo, G.; Fusiana, L. *J. Chem. Phys.* **1998**, *108*, 1377.
(10) Sverdlov, L. M.; Kovner, M. A.; Krainov, E. P. *Vibrational Spectra of Polyatomic Molecules*; Wiley: New York, 1974, and references therein.
(11) Herrebout, W. A.; Everaert, G. P.; Van der Veken, B. J.; Bulanin, M. O. *J. Chem. Phys.* **1997**, *107*, 8886.
(12) Van der Veken, B. J. *J. Phys. Chem.* **1996**, *100*, 17436.
(13) Gutman, V. *The Donor−Acceptor Approach* to Molecular Interactions; Plenum Press: New York, 1988.
(14) Herrebout, W. A.; Everaert, G. P.; van der Veken, B. J. Unpublished results.
(15) Tokhadze, K. G.; Tkhozheskaya, N. A. *J. Mol. Struct.* **1992**, *270*, 351.
(16) Everaert, G. P.; Herrebout, W. A.; Van der Veken, B. J.; Lundell, J.; Räsänen, M. *Chem. Eur. J.* **1988**, *4*, 321.
(17) Foresman, J. B.; Keith, T. A.; Wiberg, K. B.; Snoonian, J.; Frisch, M. J. *J. Phys. Chem.* **1996**, *100*, 16098.
(18) Stolov, A. A.; Herrebout, W. A.; Van der Veken, B. J. *J. Am. Chem. Soc*. **1998**, *120*, 7310.
(19) Jonas, V.; Frenking, G.; Reetz, M. T. *J. Am. Chem. Soc.* **1994**, *116*, 7714.
(20) Rayen, Y. M.; Sordo, J. A. *J. Phys. Chem. A.* **1997**, *101*, 7414.
(21) Suares, D.; Sordo, T. L. *J. Phys. Chem.* **1996**, *100*, 13462.
(22) Wales, D. J.; Popelier, P. L. A.; Stone, A. J. *J. Chem. Phys.* **1995**, *102*, 5551.
(23) Stone, A. J.; Dullweber, A.; Popelier, P. L. A.; Wales, D. J. *Orient*: A program for studying interactions between molecules, version 3.2; University of Cambridge, Cambridge, U.K.
(24) Schmidt, M. W.; Baldridge, K. K.; Boatz, J. A.; Elbert, S. T.; Gordon, M. S.; Jensen, J. H.; Koseki, S.; Matsunaga, N.; Nguyen, K. A.; Su, S. J.; Windus, T. L.; Dupuis, M.; Montgomery, J. A. *J. Comput. Chem.* **1993**, *14*, 1347.
(25) Van der Veken, B. J.; Sluyts, E. J. *J. Phys. Chem*. A **1997**, *101*, 9070.